JOURNAL OF THEORETICAL AND APPLIED MECHANICS
61, 2, pp. 233-244, Warsaw 2023
https://doi.org/10.15632/jtam-pl/160063

NUMERICAL STUDY ON COMPRESSION PROPERTIES OF SEMI-REENTRANT FILLED TUBULAR STRUCTURES

Dongquan Wu, Dinghe Li

Sino-European Institute of Aviation Engineering, Civil Aviation University of China, Tianjin, China

Corresponding author Dongquan Wu, e-mail: dqwu@cauc.edu.cn

Zhiqiang Zhang

Institute of Aviation Engineering, Civil Aviation University of China, Tianjin, China

Jiacheng Chen

The 18th Research Institute, China Electonics Technology Group Corporation, China

In this study, a semi-reentrant structure (SR) filled with different tubular structures, including tube, triangular and rectangle structures were designed. The tubular structures were perfectly assembled into semi-reentrant cells to avoid swaying in the semi-reentrant cell. The geometric relations and relative density for these structures were established. For the out-of-plane and in-plane compressions, SR filled tubular structures exhibited different deformation patterns compared to those of SR or pure fillers. A constraint effect was found between the filler tubular and container SR. With fillers contained inside the SR structures, the plateau stresses for three conditions were all promoted compared to those of SR. The best out-of-plane compression resistance occurred in the SR filled rectangle which might be caused by larger interaction areas between the SR and rectangular structures. The (specific) energy absorption of the SR filled tube compressed out-of-plane was the largest. The peak and plateau stress of the SR filled triangle was the largest compared to other structures when compressed in plane due to stability of the triangle. It was found that the plateau stress, energy absorption and specific energy absorption of SR filled triangle was the largest, while that of SR filled rectangle was the lowest.

Keywords: semi-reentrant (SR) structure, tubular fillers, out-of-plane, in-plane compression

1. Introduction

Skeletal or cellular structures with lightweight advantages, such as honeycomb with a positive Poisson's ratio, have been widely applied in the industry because of its outperformed mechanical properties and the perfect weight-to-cost ratio (Lu and Yu, 2003). Different from hexagonal honeycomb structures, auxetic structures with negative Poisson's ratios (Wang *et al.*, 2018b), such as Reentrant structures, exhibit synclastic curvature (Sevtsuk and Kalvo, 2014) and many superior mechanical properties (Wang *et al.*, 2018b). Another semi-reentrant structures are hybrids of hexagonal Honeycomb cells and Reentrant cells (see Fig. 1). A semi-reentrant structure exhibits zero Poisson's ratio in one in-plane direction and a higher elastic modulus in the other direction. It shows monoclastic surfaces (Davini *et al.*, 2017) when bending out-of-plane, thus it is suitable for applications with cylindrical shapes (Grima *et al.*, 2010). A lot of studies have focused on mechanical properties of these basic skeletal structures (Dong *et al.*, 2019). They have been used to develop components with better properties in the aerospace or automotive industries (Novak *et al.*, 2016). Although these structures have many advantages in applications, as lightweight, with good impact resistance or other properties, there is still an increasing requirement for a more superior enhancement in mechanical properties, especially about safety in the

aerospace or automotive industries. For safety reasons, in aerospace or automotive applications the large impact energy is always unwelcome and needs to be minimized or even dissipated, and crashworthiness is one of the most important properties to characterize this phenomenon. To achieve this purpose, many investigations have been conducted to create new geometrical configurations with excellent energy absorption capacity based on a honeycomb-shaped structure (Wang and Liu, 2019). It is widely known that the energy absorption of honeycomb structures depends on the non-linear plastic collapse of a unit cell with a thin wall (Wang and Liu, 2019). Hence, promoting energy absorption capacity of the unit cell could be effective in improving the energy absorption of the whole structure. For this aim, researchers have tried to fill foam materials into the spare space of honeycomb structures (Qin *et al.*, 2018) or used a double sidewall configuration. The latter method consists in filling skeletal structures into the unit cell (Wang and Liu, 2019).

Many investigations have been focused on filling foam materials into the spare space of outside container structures. The filled foam materials generally include polyurethane-foam (Yan *et al.*, 2014) or polyurethane closed-cell foam (Palanivelu *et al.*, 2010). Besides, glass/polyester composite, aluminum, lattice composite and CFRP tubes (Hussein *et al.*, 2018) have been used as the outside container materials. For geometrical configurations of the container structures, most are about tubular structures, such as thin-walled squares, circular/cylindrical, conical or hat sections tubes, and honeycomb or reentrant structures (Wang *et al.*, 2019) as well as grooved, tapered multi-cells (Wang *et al.*, 2018a). By filling foam materials into the container structure, the energy absorption ability of the structure would be substantially enlarged (Wang and Liu, 2019). However, there are still some disadvantages for filling foam materials into tubular structures, for example, to improve energy absorption, the structure should be fabricated into a long strip shape which may cause a waste of the structural space, cause an obvious increase of the structure weight and promote buckling rather than gradual folding deformation.

Therefore, to mostly utilize the hollow space of skeletal cells and to dissipate more plastic energy, filling skeletal structures into the unit cell has been proposed without sacrifice to the stability of the crash force or being lightweight. By now, there are some studies (Wang, 2019) about honeycomb filled skeletal structures. Al Antali *et al.* (2017) studied the influence of CFRP tubular-array density on specific energy absorption and characterized the dynamic response of the honeycomb core containing CFRP tubes and the rate-sensitivity. The advantages like simple preparation process and cost-effective energy absorption in dynamic applications were found. Sun *et al.* (2016) found that by incorporating an aluminium honeycomb into circular CFRP tubes, the composite structure outperformed pure aluminium honeycomb at quasi-static rates of strain, but its specific energy absorption would slightly decrease compared to the pure CFRP tubes. By filling aluminum honeycomb into square CFRP tubes, Hussein *et al.* (2016) also drew a similar conclusion after conducting experiments for a wide range of strain rates. Wang *et al.* (2019) and Wang and Liu (2019) studied out-of-plane compression performances of honeycomb cells filled with circular aluminum tubes (Wang and Liu, 2019) or CFRP tubes (Wang and Liu, 2018) (HFCT), and investigated the influence of tube fillers on deformation modes, energy absorption and interaction effects between the internal and outside container. Liu *et al.* (2018) also investigated the blast resistance performances of a sandwich panel filled with HFCT core, in which a considerable mass efficiency improvement concerning deflection resistance could be obtained.

In this study, a semi-reentrant structure filled with different skeletal structures, including tube, triangular and rectangular tubular structures were designed. To ensure the skeletal tube to be perfectly assembled into semi-reentrant cells and to avoid the oblique loadings or swaying of the skeletal tube in the semi-reentrant cell, the geometric relations of these structures were accurately calculated, and their relative density was also established. The out-of-plane and in--plane compression in two directions of these structures were investigated and compared. The

deformation mechanisms, stress against strain variations, plateau stress, densification strain and (specific) energy absorption were characterized and analyzed.

Table 1. Summary of geometrical details of different structures

Structures	Geometrical illustration	Parameters	Relative density ρ_c/ρ_A
Semi-reentrant (SR)	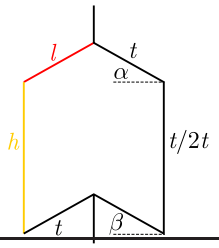	l – inclined arm length h – vertical arm length $t, 2t$ – cell wall thickness d – thickness of structure α, β – angles between arms $t = 0.08\,\text{mm}$ $\alpha = \beta = 30°$	$\dfrac{t\left(l + l\dfrac{\cos\alpha}{\cos\beta} + h\right)}{l\cos\alpha(l\sin\alpha + 2h - l\cos\alpha\tan\beta)}$
SR filled tube (SR-TU)	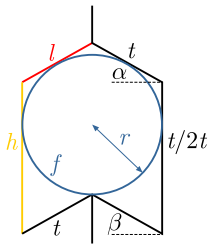	$r = 1\,\text{mm}$ – radius of circle f – cell wall thickness of filler $f = 0.008\,\text{mm}$ $l = \dfrac{r}{\cos\alpha} = \dfrac{2r}{\sqrt{3}}$ $h = \dfrac{r}{\cos\alpha} + r = \dfrac{2r}{\sqrt{3}} + r$	$\dfrac{t\left(l + l\dfrac{\cos\alpha}{\cos\beta} + h\right) + 2\pi r f}{l\cos\alpha(l\sin\alpha + 2h - l\cos\alpha\tan\beta)}$
SR filled triangle (SR-TR)	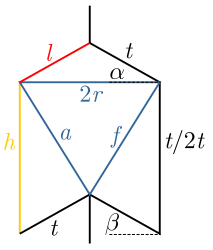	$2r = 2\,\text{mm}$ – length of edge 1 a – length of edge 2 and 3 $a = \sqrt{h^2 + l^2 - 2hl\cos\left(\dfrac{\pi}{2} - \beta\right)}$ $= r\sqrt{\dfrac{7 + 2\sqrt{3}}{3}}$	$\dfrac{t\left(l + l\dfrac{\cos\alpha}{\cos\beta} + h\right) + (2r + 2a)f}{l\cos\alpha(l\sin\alpha + 2h - l\cos\alpha\tan\beta)}$
SR filled rectangle (SR-RE)	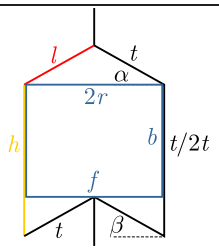	$2r = 2\,\text{mm}$ – length of edge 1 b – length of edge 3 $b = \sqrt{a^2 - r^2}$ $= r\sqrt{\dfrac{4 + 2\sqrt{3}}{3}}$	$\dfrac{t\left(l + l\dfrac{\cos\alpha}{\cos\beta} + h\right) + (4r + 2b)f}{l\cos\alpha(l\sin\alpha + 2h - l\cos\alpha\tan\beta)}$

2. Out of plane compression of semi-reentrant filled tubular structures

For compression simulation in Abaqus, width and height of the rigid compression walls are 25 mm and 25 mm, respectively, and thickness of the compression wall is 2 mm. A velocity of 50 mm/s is used to compress the structures. The cell wall thickness of SR is $t = 0.08$ mm, and the wall thickness of tubular fillers is $f = 0.008$ mm. In the simulation, the material properties of Al 3003 are used, as shown in Table 2, and the hardening of Al 3003 in quasi-static compression are considered as typical isotropic hardening, which is very commonly used for metal plasticity calculations, and it is simple and suitable for quasi-static compression conditions. Abaqus provides an isotropic hardening model that is useful for cases involving gross plastic straining or in cases where the straining at each point is essentially in the same direction in strain space throughout the analysis. The SR structures and filled structures are both built as shell models.

A specific velocity is applied in the reference point of the top grip, and the reference point of the bottom rigid grip is totally fixed. Two rigid grips are meshed with C3D8R solid elements, and the semi-reentrant structure are meshed by SR4 shell elements. The frictionless contact between the rigid grips and cell structures was introduced into Abaqus.

The stresses are calculated by the reaction forces F of the rigid grip section (S is the area of grip section, so stress is σ_1 or $\sigma_2 = F/S$). Strains $\varepsilon = U/d$ are computed from the displacements U of the top grip divided by thickness d of the structure (as shown in Fig. 1).

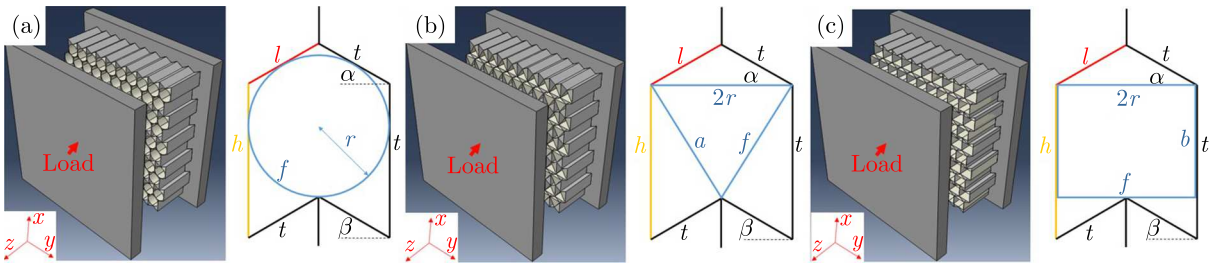

Fig. 1. Geometrical illustration of semi-reentrant structures filled with: (a) tube (SR-TU), (b) triangular (SR-TR), (c) rectangle (SR-RE) skeletal structures

Table 2. Mechanical properties of Al 3003

Materials	Elastic modulus [MPa]	Yield strength [MPa]	Ultimate strength [MPa]	Poison's ratio	Mass density ρ_A [kg/m^3]
Al 3003	70000	185	267	0.33	2700

2.1. SR filled tube structure

Figure 2 depicts deformation contours of SR, SR filled tube, SR filled triangle and SR filled rectangle compressed out-of-plane. For the SR structure, the deformation is focused on the central position in the out-of-plane direction. There is nearly no expansion in the in-plane direction of the cells. The SR filled tube exhibits a different deformation pattern compared to that of SR because the constraint effect is verified between the inner tube and the outer SR. With the influence of the filled tube, the SR filled tube deforms from the bottom section like the tube itself rather than from the middle side. And with the restriction of SR, the expansion of cells in the in-plane direction is not obvious. The SR filled triangle deforms from the top section, which is different from that of SR (deforms from the middle section), and there is an unobvious expansion of the cells in the in-plane direction due to the restriction of SR, and it could be observed that for the filled triangle, its collapse mode is compelled by the outside SR structure. The SR filled rectangle deforms both near the top and bottom sections, which is different from that of SR (deforms from middle section), and there is an unobvious expansion of the cells in the in-plane direction due to the restriction of SR, and a competitive collapse mode between the filled rectangle and outside SR is also observed.

Besides, it is concluded that the SR structure initially deforms from the middle section, and the SR filled tube deforms from the bottom side, the SR filled triangle deforms from topside, while the SR filled rectangle deforms both near the top and bottom sections, and there is no obvious expansion of the cells in the in-plane direction due to the restriction of SR.

Figure 3 compares the nominal stress versus strain curves for different structures. With fillers contained inside the SR structures, the plateau stresses for the three conditions are all promoted compared to those of SR. The plateau stress could be sorted as SR filled rectangle > SR filled tube > SR filled triangle > SR. Moreover, the densification strain could be ordered as: SR filled triangle > SR filled rectangle > SR filled tube > SR. A better compression resistance or larger plateau stress of the SR filled rectangle may be caused by larger interaction areas between the SR and rectangle structures, which will enhance the resistance of compressed deformation.

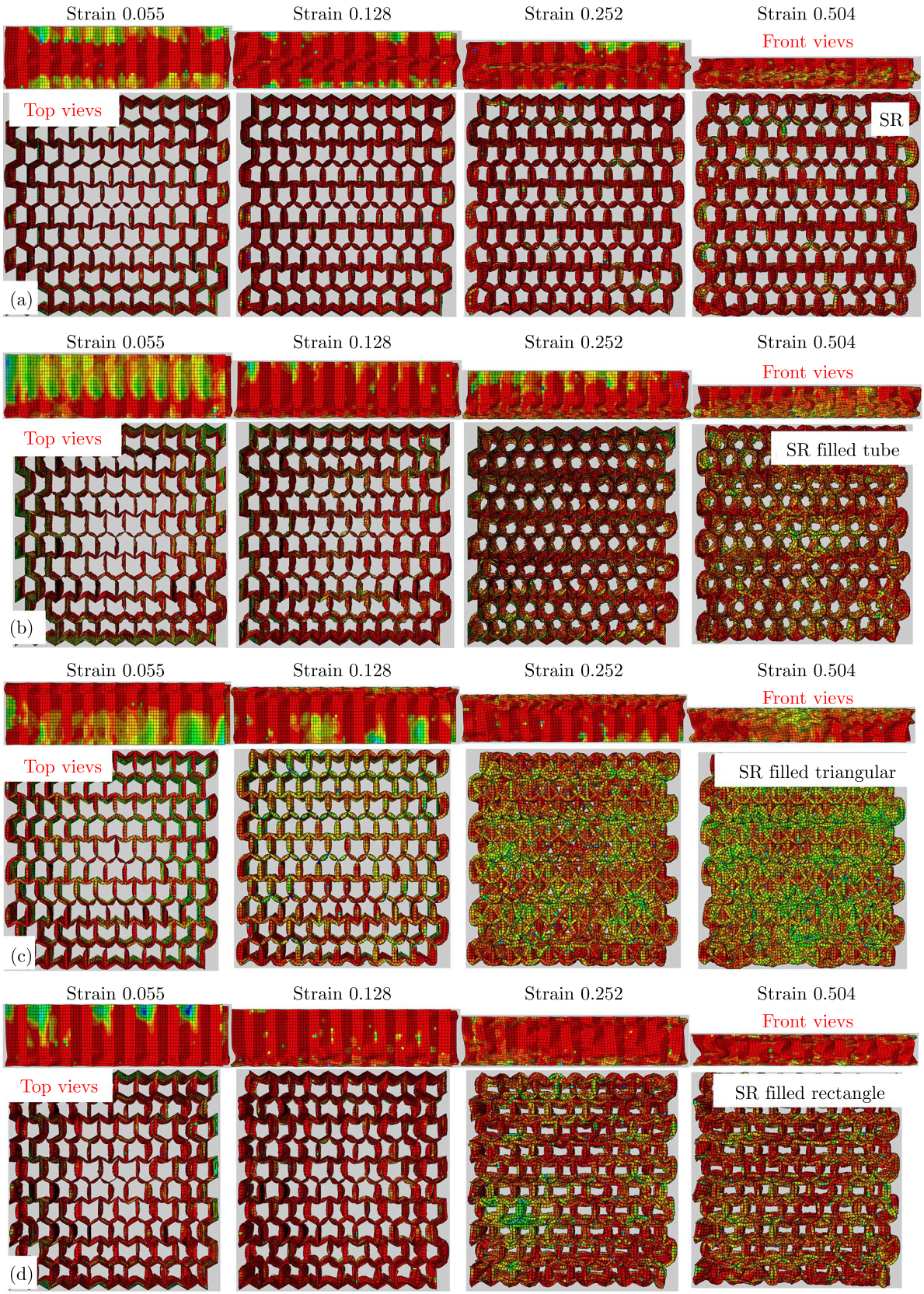

Fig. 2. Deformation contours of (a) SR, (b) SR-TU, (c) SR-TR, and (d) SR-RE

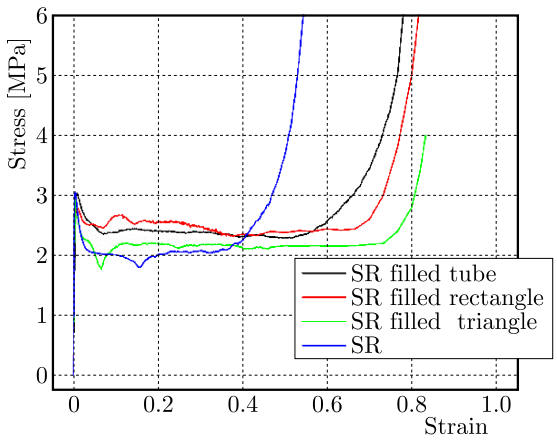

Fig. 3. Comparison of stress-strain curves among semi-reentrant structures with different fillers

Table 3 compares mechanical properties of SR filled different tubular structures. It is found that the energy absorption of SR filled tube is the largest, so is the specific energy absorption. The energy absorption and specific energy absorption have a similar order: SR filled tube > SR filled rectangle > SR filled triangular > SR.

Table 3. Mechanical properties of SR filled different tubular structures

	SR	SR-TU	SR-TR	SR-RE
Plateau stress σ_m [MPa]	2.06	2.43	2.4	2.5
Densification strain	0.54	0.866667	0.833333	0.833333
Energy absorption E [mJ]	1.1124	2.106	2	2.083333
Mass [Kg]	6.50E-04	7.31E-04	7.24E-04	7.24E-04
Specific energy absorption E_m [mJ/Kg]	1711.39	2880.99	2762.431	2877.53

3. In-plane compression of semi-reentrant filled tubular structures

For the in-plane compression of the structure, the rigid compression wall is similar to that for the out-of-plane compression. The structure is compressed along the x- or y-direction in the plane.

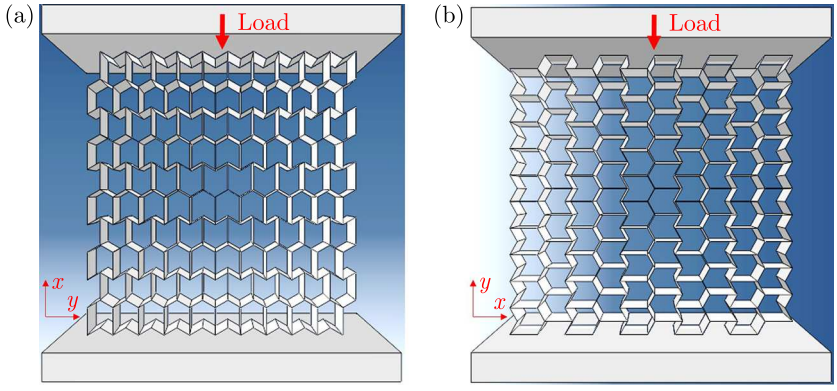

Fig. 4. Geometrical illustration of semi-reentrant structures compressed along x- or y-directions

The stresses are also calculated by the reaction forces F of the connection area between the rigid grip and structure S (so stress is σ_1 or $\sigma_2 = F/S$). Strains $\varepsilon = U/\text{width}$ are computed

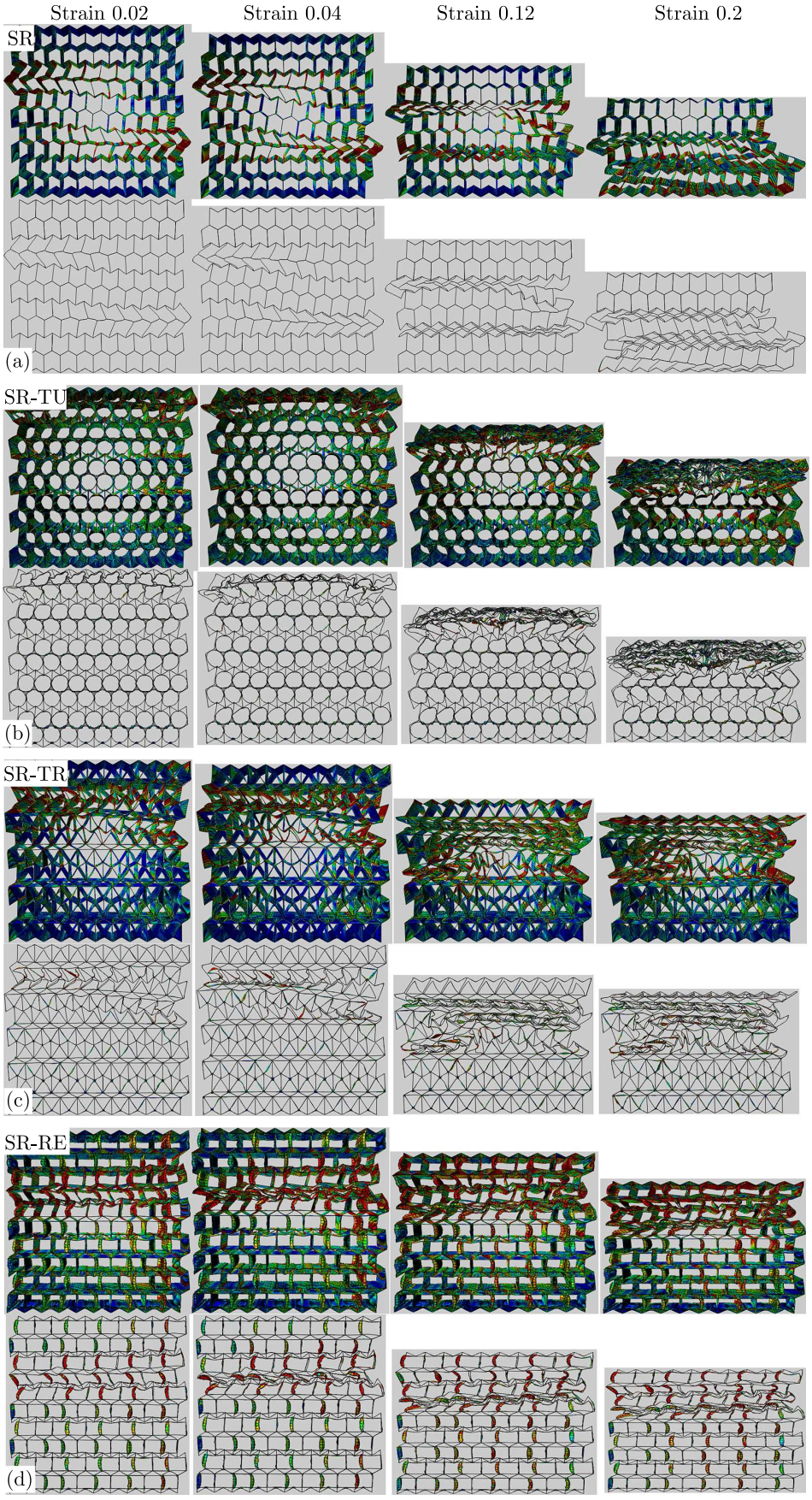

Fig. 5. Deformation contours of (a) SR, (b) SR-TU, (c) SR-TR and (d) SR-RE compressed in x-direction

from the displacements U of the top grip divided by width (compressed in x-direction) or height (compressed in y-direction) of structure (as shown in Fig. 4).

Figure 5 compares deformation contours for different structures compressed in the x-direction. For the SR structure, the deformation initially occurrs among the middle section, and with the compression distance increasing the middle and bottom sections fail and get stacked up together like a wave shape. The top section of SR keeps a good shape until the final deformation.

For the SR filled tube, the main deformation is accumulated on the top section layer by layer, and the bottom part keeps stable with few distortions. For the SR filled triangle, the major distortions are focused below the top layers, and the top layer shows a triangular shape in a long compression distance. Due to stability of the triangle, the bottom layers are very stable with nearly no deformation for the early compression process. In the SR filled rectangle, most of the deformation is located near the top layers, and the other layer is generally deformed into a rectangular shape as the compression process goes.

Figure 6 compares the nominal stress versus strain curves for different structures compressed in the x-direction. It could be found that SR with fillers will have a larger peak stress and plateau stress compared to those of the SR structures, especially for the SR filled triangle, which has better stability in the in-plane direction. The stability of the rectangular structure is also worse than that of the tube. Thus, the peak and plateau stress of these structures could be sorted as: SR-TR > SR-TU > SR-RE > SR.

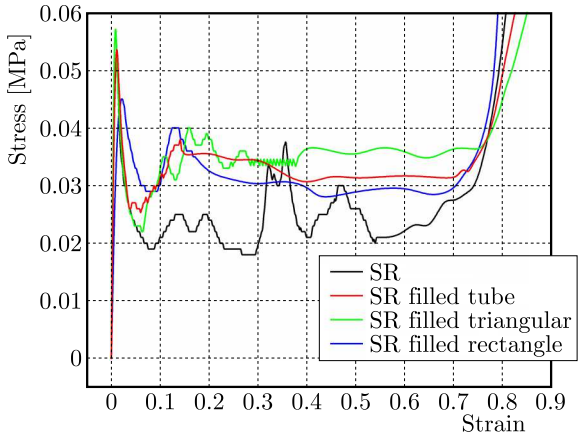

Fig. 6. Comparison of stress-strain curves among SR structures with different fillers in the x-direction

Table 4 compares the mechanical properties of SR filled different tubular structures when compressed in the x-direction. It is found that the plateau stress, energy absorption and specific energy absorption of the SR filled triangle are the largest, while these of SR filled rectangle are the lowest.

Table 4. Mechanical properties of SR filled different tubular structures compressed in x-direction

	SR	SR-TU	SR-TR	SR-RE
Plateau stress σ_m [MPa]	0.022	0.031	0.05	0.028
Densification strain	0.8	0.81	0.8	0.79
Energy absorption E [mJ]	0.0176	0.02511	0.04	0.02212
Mass [Kg]	6.50E-04	7.31E-04	7.24E-04	7.24E-04
Specific energy absorption E_m [mJ/Kg]	2.71E+01	3.44E+01	5.52E+01	3.06E+01

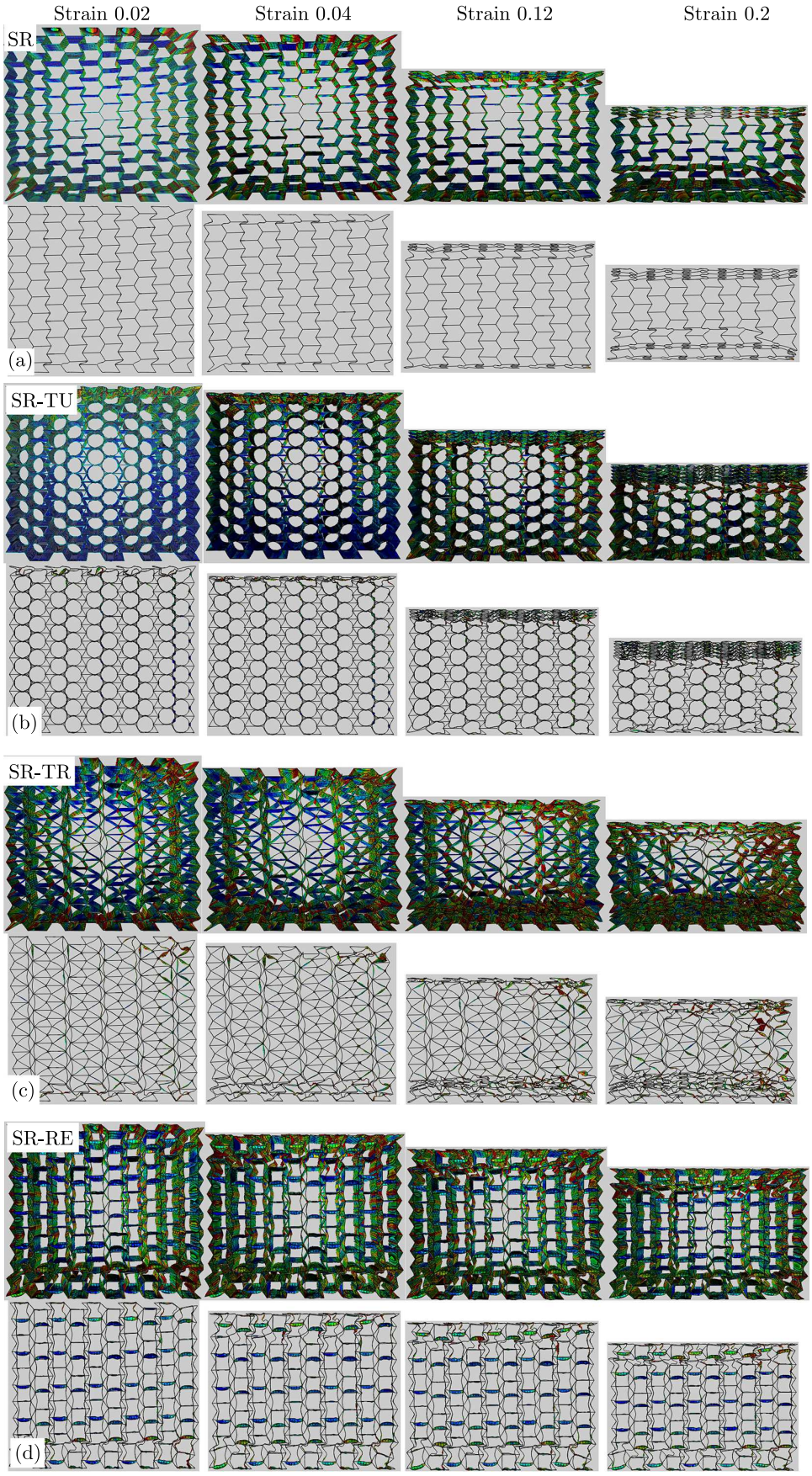

Fig. 7. Deformation contours of (a) semi-reentrant structures, (b) SR-TU, (c) SR-TR and (d) SR-RE compressed in the y-direction

Figure 7 compares deformation contours of different structures compressed in the y-direction. For the SR structure, the deformation occurs on the top and bottom sections, and the middle section is stable. The top section of SR keeps a good shape until the final deformation.

For the SR filled tube, the main deformation is accumulated on the top section layer by layer, and the bottom layer may deform a little as the compression increases. For the SR filled triangle, the major distortions are focused on the bottom layers, and a part of the top layer deforms above some compression strain load. The middle layers are very stable with nearly no deformation due to stability of the triangle. For the SR filled rectangle, most of the deformation is located near the top and bottom layers, and the other layers are already deformed into a rectangular shape.

Figure 8 compares the nominal stress versus strain curves for different structures compressed in the y-direction. It is also indicated that SR with fillers will have larger peak and plateau stressed compared to those of the SR structures, especially for the SR filled triangle. Hence, the peak and plateau stresses of these structures could be also sorted as: SR-TR > SR-TU > SR-RE > SR.

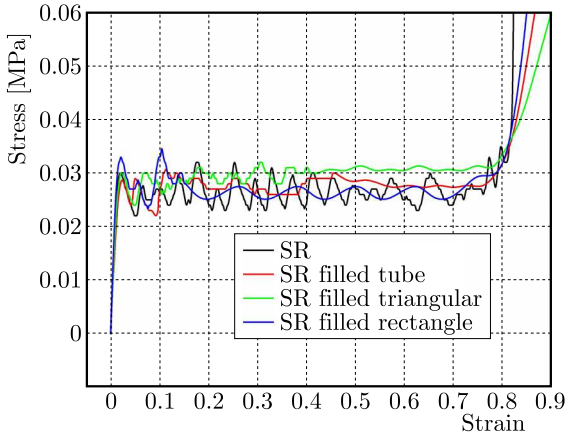

Fig. 8. Comparison of stress-strain curves among SR with different fillers in the y-direction

Table 5 compares mechanical properties of SR filled different tubular structures when compressed in the y-direction. It is found that the plateau stress, energy absorption and specific energy absorption of the SR filled triangle are the largest, while these of the SR filled rectangle are the lowest.

Table 5. Mechanical properties of SR filled different tubular structures compressed in y-direction

	SR	SR-TU	SR-TR	SR-RE
Plateau stress σ_m [MPa]	0.021	0.028	0.03	0.026
Densification strain	0.85	0.87	0.88	0.86
Energy absorption E [mJ]	0.01785	0.02436	0.0264	0.02236
Mass [Kg]	6.50E-04	7.31E-04	7.24E-04	7.24E-04
Specific energy absorption E_m [mJ/Kg]	2.75E+01	3.33E+01	3.65E+01	3.09E+01

4. Conclusion

In this study, semi-reentrant structures filled with different skeletal structures, including a tube, triangle and rectangle were designed. The out-of-plane and in-plane compression in two directions

of these structures were investigated and compared. The main conclusions are summarized as follows.

- For the out-of-plane compression, SR-TU exhibited a different deformation pattern compared to that of SR. SR initially deformed from the middle section, and SR-TU from the bottom side, SR-TR from topside, while SR-RE deformed both near the top and bottom sections, and there was no obvious expansion of the cells in the in-plane direction, meaning that a constraint effect appeared between the tubular filler and SR container. With the fillers contained, the plateau stresses for three conditions were all promoted compared to those of SR. The plateau stress were sorted as: SR-RE > SR-TU > SR-TR > SR. The densification strain was ordered as: SR-TR > SR-RE > SR-TU > SR. A better compression resistance or larger plateau stress of SR-RE may be caused by larger interaction areas between the SR and rectangular structures. The (specific) energy absorption of SR-TU was the largest.
- For the in-plane compression in the x-direction, SR initially deformed around the middle section and then the bottom failed in a wave-way. For SR-TU, the main deformation was accumulated on the top section layer by layer, while the bottom part kept stable. For SR-TR, major distortions were focused below the top layers and the top layer was compressed into a triangular shape after a large loading. Due to triangular stability, the bottom layers were quite stable at the initial stage. For SR-RE, deformation was located around the top layers and other layers were generally deformed into a rectangular shape. For the in-plane compression in the y-direction, SR deformed on the top and bottom sections, and its middle section was stable. For SR-TU, deformation was similar to that in the x-direction. For SR-TR, major distortions were focused on the bottom layers, and some top layers deformed after some compression strain, while the middle layers were stable. For SR-RE, deformation was located near the top and bottom layers. SR with fillers would have larger peak and plateau stresses compared to those of SR structures, especially for SR-TR. The peak and plateau stress of these structures could be sorted as: SR-TR > SR-TU > SR-RE > SR. The plateau stress, energy absorption and specific energy absorption of SR-TR were the largest, while that of SR-RE were the lowest.

Acknowledgement

The authors would like to acknowledge the support from the Scientific Research Program of Tianjin Education Commission (Grant No. 2021KJ053) and Aviation Science Foundation of China (Grant No. 20200038067001).

References

1. Al Antali A., Umer R., Zhou J., Cantwell W.J., 2017, The energy-absorbing properties of composite tube-reinforced aluminum honeycomb, *Composite Structures*, **176**, 630-639
2. Davini C., Favata A., Micheletti A., Paroni, R., 2017, A 2D microstructure with auxetic out-of-plane behavior and non-auxetic in-plane behaviour, *Smart Materials and Structures*, **26**, 12, 125007
3. Dong Z., Li Y., Zhao T., Wu W., Liang J., Xiao D., 2019, Experimental and numerical studies on the compressive mechanical properties of the metallic auxetic reentrant honeycomb, *Materials and Design*, **182**, 108036
4. Grima J.N., Oliveri N., Attard D., Ellul E., Gatt G., Cicala N., Recca G., 2010, Hexagonal honeycombs with zero Poisson's ratios and enhanced stiffness, *Advanced Engineering Materials*, **12**, 9, 855-862

5. Hussein R.D., Dong R., Lu G., Thomson R., 2018, An energy dissipating mechanism for crushing square aluminium/CFRP tubes, *Composite Structures*, **183**, 643-653
6. Hussein R.D., Ruan D., Lu G., Sbarski I., 2016, Axial crushing behaviour of honeycomb-filled square carbon fibre reinforced plastic (CFRP) tubes, *Composite Structures*, **140**, 166-179
7. Liu J., Wang Z., Hui D., 2018, Blast resistance and parametric study of sandwich structure consisting of honeycomb core filled with circular metallic tubes, *Composites Part B: Engineering*, **145**, 261-269
8. Lu G., Yu T.X., 2003, *Energy Absorption of Structures and Materials*, Elsevier, 1-424
9. Novak N., Vesenjak M., Ren Z., 2016, Auxetic cellular materials – a review, *Strojniški Vestnik – Journal of Mechanical Engineering*, **62**, 9, 485-493
10. Palanivelu S., Paepegem W.V., Degrieck J., Vantomme J., Kakogiannis D., Ackeren J.V., Hemelrijck D.V., Wastiels J., 2010, Comparison of the crushing performance of hollow and foam-filled small-scale composite tubes with different geometrical shapes for use in sacrificial cladding structures, *Composites Part B: Engineering*, **41**, 6, 434-445
11. Qin Q., Zhang W., Liu S., Li S., Zhang J., Poh L.H., 2018, On dynamic response of corrugated sandwich beams with metal foam-filled folded plate core subjected to low-velocity impact, *Composites Part A: Applied Science and Manufacturing*, **114**, 107-116
12. Sevtsuk A., Kalvo R., 2014, A freeform surface fabrication method with 2D cutting, *2014 Proceedings of the Symposium on Simulation for Architecture and Urban Design*, 109-116
13. Sun G., Li S., Liu Q., Li G., Li Q., 2016, Experimental study on crashworthiness of empty/aluminum foam/honeycomb-filled CFRP tubes, *Composite Structures*, **152**, 969-993
14. Wang T., Wang L., Ma Z., Hulbert G.M., 2018b, Elastic analysis of auxetic cellular structure consisting of re-entrant hexagonal cells using a strain-based expansion homogenization method, *Materials and Design*, **160**, 284-293
15. Wang Y., Lai H., Ren X.J., 2019, Enhanced auxetic and viscoelastic properties of filled reentrant honeycomb, *Physica Status Solidi*, **257**, 1900184
16. Wang Z., 2019, Recent advances in novel metallic honeycomb structure, *Composites Part B: Engineering*, **66**, 731-741
17. Wang Z., Liu J., 2018, Mechanical performance of honeycomb filled with circular CFRP tubes, *Composites Part B: Engineering*, **135**, 232-241
18. Wang Z., Liu J., 2019, Numerical and theoretical analysis of honeycomb structure filled with circular aluminum tubes subjected to axial compression, *Composites Part B: Engineering*, **165**, 626-635
19. Wang Z., Liu J., Yao S., 2018a, On folding mechanics of multi-cell thin-walled square tubes, *Composites Part B: Engineering*, **132**, 17-27
20. Yan L., Chouw N., Jayaraman K., 2014, Lateral crushing of empty and polyurethane-foam filled natural flax fabric reinforced epoxy composite tubes, *Composites Part B: Engineering*, **63**, 15-26

Manuscript received September 28, 2022; accepted for print December 14, 2022